ChemPubSoc Europe

DOI: 10.1002/celc.201300200

Oxygen-Terminated Diamond Electrodes in Alkaline Media: Structure and OH Generation

Paola M. Quaino*[a] and Wolfgang Schmickler[b]

The structure and energetics of two types of oxygen-terminated diamond surfaces, the keto and ether configurations, were investigated by density functional theory. To explore OH generation, we studied the approach of a hydroxyl radical to these surfaces. The OH radical strongly interacted with the ether-type surface, whereas the radical was repelled in the keto configuration. The kinetics of OH generation in alkaline solutions ($OH^- \leftrightarrow OH + e^-$) on oxygen-terminated diamond electrodes was investigated in light of the theory of catalyzed electron transfer. Our results suggested that the electron transfer occurs in the outer-sphere mode with an activation energy of 0.5 eV.

1. Introduction

■■Please provide academic titles (Prof./Dr.) for each author and the email address of the corresponding author. Please check references - ensure that they are cited in numerical order■■Not only does diamond form decorative crystals, but its surfaces are also of great interest in many fields such as optical coatings, electronic devices, biochemistry, and environmental chemistry. In the area of electrochemistry, in particular, boron-doped diamond (BDD) exhibits unique properties as an electrode material, including a wide potential window,[1,2] low double-layer capacitance, chemical inertness, and structural stability. For a comprehensive overview, see ref. [3] and the references cited therein.

The electrochemical properties of BDD electrodes are determined by their surface composition. Usually, a diamond structure exhibits hydrogen[3–5] or oxygen[3,6,7] terminations. The latter can be obtained by several methods such as electrochemical oxidation and O_2-plasma treatment.[3] The surface groups generated may depend on the crystal face; for instance, hydroxyl groups could be found on (111) materials, whereas two chemical bonds are found for a single carbon atom in the first layer of an ideal (100) diamond surface; hence, carbonyl (top) and ether (bridge) groups are expected. An advantage of surface oxidation treatment is that it changes the electrochemical nature of the diamond electrodes and facilitates their functionalization for several applications. Water treatment[8,9] and fuel cells are of paramount importance, and they are two of the most investigated applications of diamond electrodes. The former exploits two features, the high overpotential for oxygen evolution and the possibility to anodically produce hydroxyl radicals in a very effective manner.[10] In the case of energy-conversion systems, the search for a promising electrocatalyst with the requirements of high electrocatalytic activity, stability, and low price has focused on metal oxides, which are mainly stable in alkaline media. In this respect, doped diamond surfaces could be used as inert and stable substrates for the deposition of nanoparticles or films.[11]

In this context and taking into account that diamond structures could be electrochemically oxidized in the oxygen evolution potential region, the present work is centered on the behavior of oxygen-terminated diamond electrodes in the presence of hydroxyl radicals to gain deeper understanding of the fundamental principles governing the involved processes. In particular, we explore the kinetics of the production of the OH radical in alkaline solutions.

[a] P. M. Quaino
Programa de Electroquímica Aplicada e Ingeniería Electroquímica (PRELINE)
Fac. de Ingeniería Química, Universidad Nacional del Litoral
Santa Fe (Argentina)

[b] W. Schmickler
Institute of Theoretical Chemistry
Ulm University, 89069 Ulm (Germany)

Methods

First-Principles Calculations

Periodic density functional theory (DFT) calculations were performed with the DACAPO code,[12] which utilizes an iterative scheme to solve the Kohn–Sham equations of DFT self-consistently. A plane-wave basis set was used to expand the electronic wavefunctions, and the inner electrons were represented by ultrasoft pseudopotentials,[13] which allow the use of a low-energy cutoff for the plane-wave basis set. Electron–electron exchange and correlation interactions were treated with the generalized gradient approximation (GGA) in the version of Perdew and Wang (PW91).[14] The parameterization of the energy cut-off and the *k*-points sampling of the Brillouin zone on the basis of the Monkhorst–Pack grid[15] was considered. Both parameters were increased systematically until the change in the absolute energy was less than 10 meV. An energy cutoff of 640 eV and a grid of (6×6×1) *k*-points were used. Spin polarizations are mentioned if considered. Dipole correction was used to avoid slab–slab interactions.[16] The relaxations were performed within the quasi-Newton minimization scheme, and the convergence criterion was achieved if the total forces were less than 0.02 eV $Å^{-1}$.

Diamond Modeling

Under vacuum, the (1 0 0) oxygen-terminated surface exhibited a (2×1) reconstruction. The behavior of OH was investigated by first-principles calculations and in light of the theory of electrocatalysis proposed and developed by Santos and Schmickler.[17–21]■■ok?■■

A (2×1) reconstructed (1 0 0) diamond surface was modeled with a slab consisting of 10 carbon layers and a vacuum region equivalent to 12 layers. Two different oxygen-terminated configurations were studied: the keto and ether configurations. In the former, each surface C atom is linked to another two C atoms by a simple bond and to an O atom by a double bond (Figure 1, right). For ether-type adsorption, the surface carbon atom is connected to O and C atoms by single bonds (Figure 1, left); oxygen atoms adsorbed at the bridge sites within two-carbon dimer row were considered.

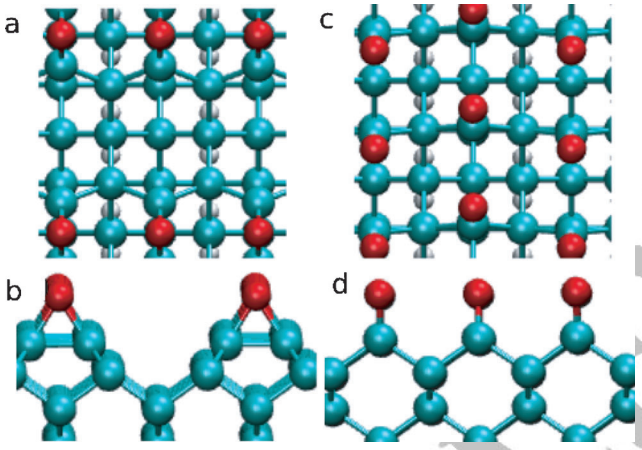

Figure 1. The O-terminated (2×1) reconstructed (1 0 0) diamond surface. Two different oxygen configurations were considered: ether and bridge position (right) and keto and atop position (left) structures. a, b) Top and side view of ether termination. C–C distance: 1.53 Å, O–C distance: 1.44 Å. c, d) Top and side view of keto termination. C–C distance: 2.52 Å, O–C distance: 1.21 Å.

To avoid dangling bonds at the truncated C–C bulk, hydrogen atoms were used to maintain sp^3 hybridization of the bottom carbon layer. The presence of hydrogen introduces changes in the electron density of the bottom layer, but according to ref. [22], H termination does not have a significant effect on the energetics of the top layer, at which the adsorption is studied.

The terminal oxygen atoms, the first carbon layer, and the H in OH were allowed to relax fully. The oxygen atom in the radical was kept fixed in all coordinates at different z distances perpendicular to the corresponding surface.

Diamond electrodes are usually highly doped to make them conductive, and boron is the most commonly used dopant. However, at practical doping levels the concentration of the dopant is so much smaller than that of the carbon atoms, and thus, its presence at the surface can be safely ignored. Therefore, we only considered the structure of pure diamond surfaces.

2. Structure and Energetics

To investigate the energetics and stability of the O-terminated structures under consideration, binding energies (E_b) were calculated relative to $O_{2(g)}$ and a reference state slab according to Equations (1) and (2):

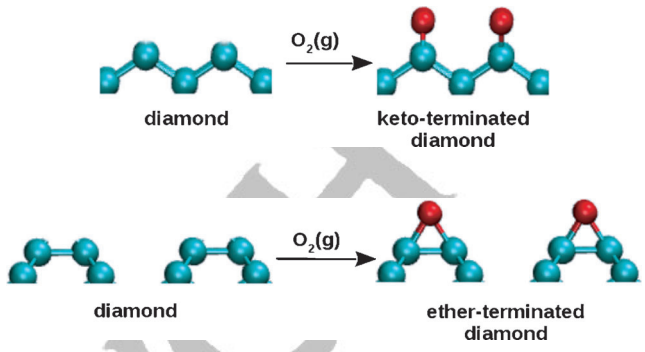

$$E_b^{keto-D} = -\frac{1}{N_O}\left\{E^T_{keto-D} - E^T_D\right\} + \frac{1}{2}E_{O_2} \quad (1)$$

$$E_b^{ether-D} = -\frac{1}{N_O}\left\{E^T_{ether-D} - E^T_D\right\} + \frac{1}{2}E_{O_2} \quad (2)$$

in which E^T_{keto-D} and $E^T_{ether-D}$ are the total energies of the O-terminated diamond surface in the keto and ether configurations, respectively; E^T_D represents the total energy of the pure (2×1) reconstructed (1 0 0) diamond surface; N_O is the number of oxygen atoms, and E_{O_2} is the total energy of the oxygen molecule in the gas phase. Because of the well-known difficulties of DFT with the oxygen molecule, we used the experimental value. Zero-point energy corrections were not included, and the energies are given at $T = 0$ K. For all the possible oxygen-termination scenarios, only the ether and keto configurations indicated in Figure 1 were investigated for our purpose.

Our results show that the oxygen in the ether configuration is energetically favorable, with a binding energy of about −5.36 eV for an oxygen-surface coverage up to 50%, with the reconstructed diamond surface preserved. Our binding energy is in good agreement with the literature (−5.68[23] and −5.35 eV[27]).■■ref 27 is cited out of order - please check and renumber■■ The ether species are bonded covalently to the carbon dimers (C–C distance = 1.53 Å) in a (2×1) reconstructed (1 0 0) diamond surface with an O–C bond distance of about 1.44 Å, again in accord with the literature data.[23–25]

Investigation of an adsorbed oxygen monolayer on the reconstructed diamond surface indicated that the lowest energy appeared if the oxygen atoms were in the keto form during cleavage of the dimer bond.■■ok?■■ Each oxygen atom is double bonded to the surface with an O–C distance of about 1.21 Å and a binding energy around −5.86 eV for 100%

oxygen-surface coverage. Unlike ether adsorption (50% oxygen coverage), in which the reconstructed diamond structure remained unchanged, in the keto adsorption (100% oxygen coverage) the diamond surface is highly perturbed, the reconstruction is lost, and the diamond surface becomes almost undistorted and forms a zigzag surface pattern with O–C–C angles deviating from the ideal structure by $\pm 20^{\circ}$ (Figure 2). Similar results were found by Petrini et al.[23] A comparison with the binding energy for a full monolayer of ether termination (−6.22 eV[23,27]) confirmed that the latter is thermodynamically more favorable than keto terminations (−5.86 eV) in accordance to refs. [23, 26–28]. Interpretation of these results suggests that in the most energetically stable structure for oxygen-terminated surfaces, the (2×1) reconstruction is lifted; comparable results were reported in ref. [27].

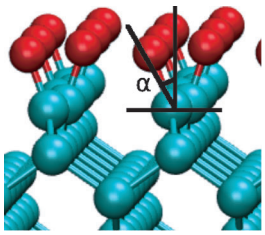

Figure 2. Optimized keto-type terminated diamond surface: the reconstruction is not preserved; α is the angle of deviation to the normal line perpendicular to the surface.

As mentioned in the Introduction, we were particularly interested in the generation of the OH radical in alkaline solution. To investigate the fate of the OH radical at the surface, we investigated its approach to an oxygen-covered surface. The corresponding energy–distance curves were also required to calculate the free-energy surface for OH generation, which will be discussed below.

Figures 3 and 4 show the behavior of OH as it approaches the oxidized diamond surface. The radical was fixed at several distances to the electrode, as described previously (see the section on Diamond Modeling). To calculate the perpendicular distance of OH to the electrode, the *z* coordinate of the oxygen atoms in the keto/ether-type termination was used as a reference.

Figure 3 exhibits the approach of OH to the keto-type terminated surface. Repulsive interactions and steric effects were detected due to high coverages and a high electronic charge concentration on the surface. Therefore, the favored situation was found at larger distances of OH from the oxidized diamond, and as expected, the energy smoothly increased with decreasing separation of OH from the electrode. For larger distances (>0.5 Å with reference to the O termination) the O–H bond remained unmodified at about 0.99 Å, whereas the O–C bond in the keto-terminated diamond slightly moved up with an O–C–C angle oscillating around 90° (Figure 3); this in turn corresponds to an almost-undistorted diamond structure.

At shorter distances (<0.5 Å) from the electrode, the formation of an unstable adsorbed H–O–O species was observed

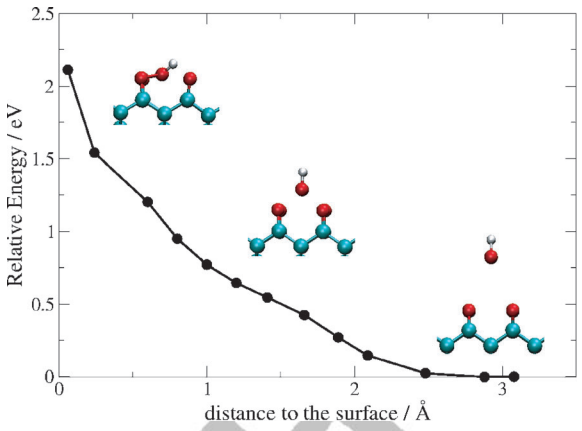

Figure 3. Initial structure: OH at 3.0 Å on an O-terminated (keto) (1 0 0)-(2×1) diamond surface. The *z* coordinate of the oxygen atoms in the keto-type termination was used as reference to calculate the perpendicular distance of OH to the surface. Final structure: OH at a *z* distance similar to that of the keto-type termination. Structural modifications were found on the surface atoms (carbon and oxygen) at shorter distances of OH to the electrode to minimize the repulsive and geometrical interactions.

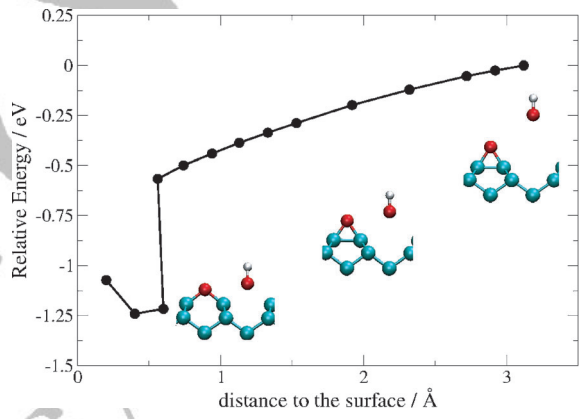

Figure 4. Initial structure: OH at 3.0 Å on an O-terminated (ether) (1 0 0)-(2×1) diamond surface. The *z* coordinate of the oxygen atoms in the ether-type termination was used as reference to calculate the perpendicular distance of OH to the surface. Final structure: OH at a *z* distance similar to that of the ether-type termination.

with the following geometrical parameters (Figure 3): O–O distance of 1.48 Å (in agreement with the reported data for the hydroperoxide species[29]), H–O distance of 0.99 Å, and O–C distance of 1.30 Å. Elongation of the O–C bond suggests that the double bond no longer exists and that a single bond was formed, although our value (1.30 Å) is rather small in comparison to an O–C single bond (≈1.43 Å[29]).

Different behavior was found if the OH approached an ether-terminated (1 0 0)-(2×1) reconstructed diamond (see Figure 4). As mentioned previously, an oxygen-surface coverage up to 50% was considered. For larger distances of the hydroxyl radical to the surface, the energy increased, and a typical reconstructed diamond was found: C–C dimer distance of 1.54 Å and C–O bond of 1.43 Å. Unlike the keto case, the most favorable scenario occurred if the OH was surrounded by ether groups at 0.4 Å (with reference to the O termination, Figure 5).

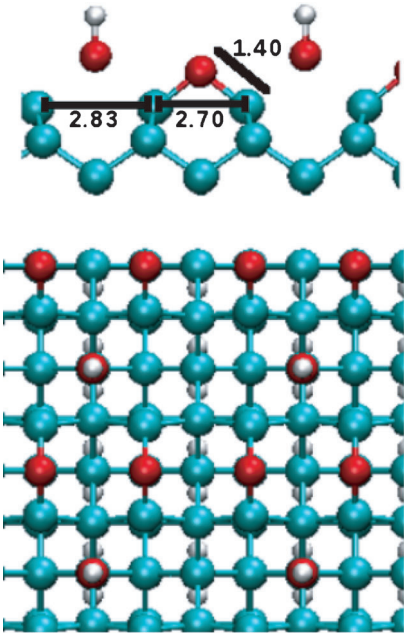

Figure 5. Optimized ether-type terminated diamond surface in the presence of OH species. Side and top views. Distances are given in Å.

The most prominent feature was the tendency to restore the diamond undistorted structure, with C–C bond lengths around 2.70 and 2.83 Å (see Figure 5) compared with 2.52 Å for an ideal C–C bond.[29]

The overall picture can be summarized as follow: several individual or combined parameters can affect the behavior of the diamond. Its structure and reactivity can be mainly modified by the surface coverage, the type of termination bond, and the environment. The diamond structure will vary between an ideal or reconstructed structure depending on which one is energetically more favorable for the system under consideration.■■ok?■■

For the sake of completeness, we additionally examined the effect of OH radicals on the H-terminated (1 0 0)-(2×1) diamond surface (hydrogen-surface coverage up to 100%). The combination of a hydroxyl radical with a terminal hydrogen leads to the formation of a water molecule plus the creation of a dangling bond in the diamond surface with a reaction energy (E_r) of about −1.8 eV. This value, which in this particular case accounts for the formation of water plus its interaction with the diamond surface, was evaluated according to Equation (3):

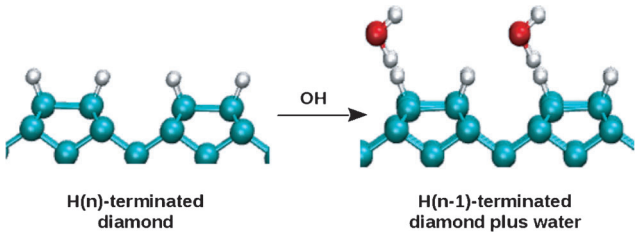

$$E_r = E_{\frac{H_2O}{D_{(nH-1)}}} - E_{D_{(nH)}} - E_{OH} \quad (3)$$

in which $E_{\frac{H_2O}{D_{(nH-1)}}}$ is the total energy of the hydrogen-terminated diamond surface that has lost one hydrogen due to the interaction with OH plus a water molecule, $E_{D_{(nH)}}$ accounts for the total energy of the H-terminated diamond surface, and E_{OH} is the total energy of the hydroxyl radical in the gas phase. Zero-point energy corrections were not included and the energies are given at $T = 0$ K.

In these circumstances, the water molecule interacts with the diamond surface at a H_{down}–diamond distance of 1.85 Å; one hydrogen points down with respect to the surface and the other one points up to preserve the H–O–H angle. The water structure remains geometrically unchanged with values of about 0.97 and 1.012 Å for the H_{up}–O and H_{down}–O distances, respectively, and 104.9° for the H–O–H angle. As expected, a subtle elongation of the bond length due to water–surface interactions was detected for the H_{down}–O bond.

Taking into account the result of our optimization procedure,[1] two highly favorable products were obtained: a water molecule and a 75% H coverage reconstructed diamond with an isolated dangling bond. The removal of a hydrogen atom reduced the electrostatic repulsion between the neighboring CH polar groups and favored the formation of an isolated dangling bond, which led to higher stability, and this is in agreement with the data reported by Zilibotti et al.[30]

3. Electrochemical Generation of the OH Radical

Because of its chemical inertness, OH radicals can be generated at BDD,[31] which in turn may serve as a useful reagent for a variety of reactions. The mechanism of OH generation depends on the pH. In acid solution, it follows Equation (4):

$$H_2O \leftrightarrow OH + H^+ + e^- \quad (4)$$

According to Kapalka et al.,[32] the standard equilibrium potential at pH 0 is about 2.38 V versus the normal hydrogen electrode■■ok?■■. In alkaline solutions the mechanism follows Equation (5):

$$OH^- \leftrightarrow OH + e^- \quad (5)$$

The standard equilibrium potential of 1.55 V for pH 14 given by Bard, Parsons, and Jordan[44] ■■ref 44 is cited out of order - please check and renumber■■agrees well with the value quoted above for acid solutions.

According to our investigations above, an OH radical can follow one of several courses: On a hydrogen-covered surface, it combines with hydrogen to form water and is lost as a re-

[1] *The initial structure used for the optimization was a OH radical at several angstroms from a H-terminated reconstructed diamond surface. Hydrogen-surface coverage: 100%. For the relaxations, the terminal hydrogen atoms, the first carbon layer, as well as the OH were allowed to be fully optimized.*

agent. On an oxygen covered surface in the ether configuration, it is strongly adsorbed. On an oxygen covered surface in the keto configuration, it is repelled at short distances. Therefore, continuous OH generation can only take place at a keto surface or at a surface coverage of 50% oxygen in the ether configuration and 50% OH coverage. In either case, further OH adsorption is no longer possible. To be specific, we investigated OH generation in alkaline solutions according to Equation (5) in the keto configuration, but the results should be very similar to those obtained in the other case.

We calculated the free-energy surface for the reaction within the framework of the theory of catalyzed electron transfer.[17,18,33] For this purpose, we needed the electronic interaction of the reactant with the electrode surface. As is evident from Figure 4, the energy of the OH radical increases strongly as it approaches the oxygen-covered surface. Therefore, the electron transfer takes place in the outer-sphere mode, with an optimal distance of about 3 Å from the surface, so we needed the interaction at distances of this order. For reactions in the outer-sphere mode, the interaction is characterized by a single interaction energy Δ,[34] which is the broadening of the reactant's valence level due to its interaction with the electrode. Values of $\Delta \geq 10^{-4}$–10^{-3} eV are sufficient to make the reaction adiabatic.

At short distances, the interaction energy Δ can directly be obtained from the density of states of the p orbital of the oxygen atom of OH. Thus, for a distance of 1.5 Å we obtained $\Delta = 0.2$ eV, and for a distance of 2.0 Å we obtained $\Delta = 0.15$ eV. At larger distances, Δ can no longer be obtained from the energy broadening, as it becomes too small. In this range, interaction energies fall off exponentially, with decay lengths of the order of 0.5 to 1 Å, so we may safely conclude that at 3 Å, the interaction is in the adiabatic range.

Solvent reorganization plays an important role in electron transfer; therefore, we investigated the solvation of HO^- near the interface. In the bulk, the solvation energy of this ion is about 4.8 eV.[37] ■■refs 35 and 36–see below–are cited out of order■■Its variation near the interface is given by the potential of mean force (pmf), which gives the work required to move the particle from the bulk towards a given position near the electrode surface. The latter was determined by molecular dynamics simulations with umbrella sampling as described in ref. [38]. The effect is comparatively small, as HO^- fits well into the water structure. Thus, at a distance of 3 Å, the distance at which the reaction takes place, the pmf is only 0.13 eV and it rises slowly towards the surface to reach a value of 0.26 eV at 2 Å. Given that this change in the solvation energy plays only a very minor role in the reaction, we do not describe the details of the simulations here but leave this to a future paper on the adsorption of OH,[39] for which its effect is more important.

The solvation energy ΔG_{sol} can be split into two parts: the energy of reorganization λ and the fast solvation energy.[40] The division is given by the Pekar factor [Eq. (6)]:[41,42]

$$\lambda = \left(\frac{1}{\varepsilon_\infty} - \frac{1}{\varepsilon_s}\right)\Delta G_{sol} \qquad (6)$$

in which ε_∞ and ε_s are the optical and the static dielectric constant, and the term in brackets is the Pekar factor, which for water is about 0.5■■ok?■■. The OH radical has a solvation energy of about 0.42 eV,[43] which must be subtracted from the solvation energy of the anion to obtain the change in the solvation energy. We note that the energy of reorganization is much larger than the energy broadening Δ, so that the latter has no effect on the energy of activation.[34]

The interfacial capacity of BDD in contact with an aqueous solution depends on the preparation and the doping, but it is always small of the order of 4 μF cm^{-2} or less,[3] as may be expected for a semiconductor. Therefore, any potential drop between the bulk of the solution and the bulk of the electrode will primarily take place within the semiconductor itself, and the electric field in the surface region of the electrolyte will be weak; therefore, it can be safely neglected in our calculations.

With this information, we performed calculations for alkaline solutions and for the case in which the reaction was in equilibrium. The resulting free-energy surface is shown in Figure 6. It

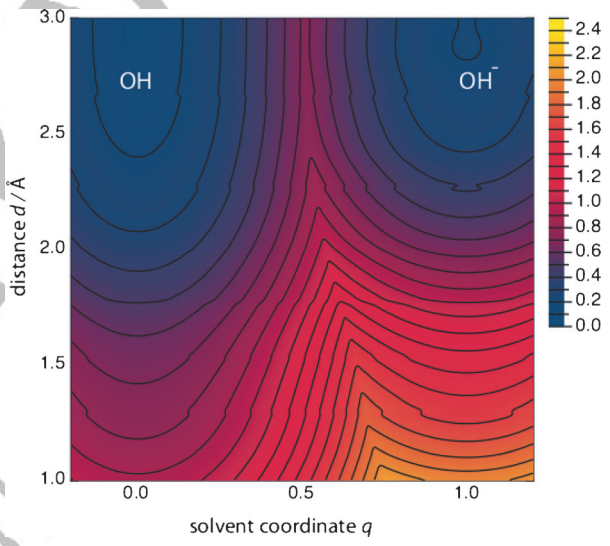

Figure 6. Free-energy surface of the generation of the OH ion at oxygen-covered diamond in the keto configuration; all energies are in eV.

was plotted as a function of the distance of the reactant from the surface and of the solvent coordinate q. The latter is familiar from the early works of Marcus[35] and Hush[36] and characterizes the state of the solvent. During the reaction, the configuration of the solvent passes from that appropriate for the HO^- anion to that for OH; in our normalization, a value q of the solvent coordinate indicates that the solvent configuration would be in equilibrium with a charge of $-q$ on the reactant. Thus, during the oxidation q passes from -1 to 0.

As was expected, the free-energy surface shows features of a typical outer-sphere electron transfer: two minima of equal depth separated by a barrier. At closer distances the reaction is less favorable, as the energies of the reactants rise. The energy of activation is about 0.5 eV, which is the value of $\lambda/4$ predicted by Marcus theory. However, our model differs significantly

from Marcus theory in another aspect. In the latter, the energy of reorganization is obtained from a simple electrostatic model equivalent to Born's formula for the energy of solvation of ions. This simple model would predict a significant decrease in the solvation as the anion approaches the surface due to the formation of an image charge on the electrode. However, our simulation showed that HO^- fits very well into the structure of water and can approach the surface with very little loss of solvation. At a distance of 3 Å, the point at which the reaction takes place, the energy of solvation of this ion is almost the same as that in the bulk.

4. Concluding Remarks

In this work, we investigated the surface structure of oxygen-terminated BDD electrodes and identified two adsorbate structures corresponding to a keto and an ether configuration. Throughout this work, our focus was on the generation of the OH radical in alkaline solutions. From a combination of DFT and molecular dynamics simulations we obtained the interaction parameters required to calculate the free-energy surface for this reaction. Specific calculations were performed for the keto configuration, but the results should be the same if the surface is covered by a stable adsorbate that does not react with the OH that is generated. Under these circumstances, the reaction is adiabatic and follows Marcus theory, with an energy of activation of about 0.5 eV.

Upon relating our work to experimental data, it should be borne in mind that the surface that we calculated is for electron exchange with the Fermi level of the electrode; this will happen if doping is so high that the semiconducting BDD is degenerate at the surface. If the doping is lower so that the top of the valence band lies below the Fermi level, the energy of activation will be higher. In this case, the reaction can be described by the theory of adiabatic reactions at semiconductors[40,45,46] by using the information given above. However, in practical applications one usually uses highly doped BDD, so that electron transfer should occur at or near the Fermi level.

A detailed comparison of our work with experimental data is not possible at this stage. Kinetic measurements of OH generation are difficult because of the short lifetime of the radical. However, our conclusion that this reaction should take place in an outer-sphere mode is in line with the suggestion of Kapalka et al.[32] that the generated OH radical interacts so weakly with BDD that it can be considered free.

Acknowledgements

Financial support by the Deutsche Forschungsgemeinschaft (Schm 344/34-1,2; Sa 1770/1-1,2; and FOR 1376) and by an exchange agreement between the DAAD and MINCYT (Argentina) are gratefully acknowledged. P.Q. and W.S. thank CONICET ■■please provide full name of DAAD, MINCYT, and CONICET■■for continued support. A generous grant of computing time from the Baden-Württemberg grid is gratefully acknowledged. It is a pleasure to acknowledge a stimulating exchange of ideas with Cristos Comninellis from ETH, Lausanne.

Keywords: carbon · density functional calculations · electron transfer · radicals · oxygen-terminated diamond

[1] F. Bouamrane, A. Tadjeddine, J. E. Butler, R. Tenne, C. Lévy-Clément, *J. Electroanal. Chem.* **1996**, *405*, 95 – 99.
[2] H. B. Martin, A. A. Argoitia, U. Landau, A. B. Anderson, J. C. Angus, *J. Electrochem. Soc.* **1996**, *143*, L133 – L136.
[3] A. Fujishima, Y. Einaga, T. Narasinga Rao, D. Tryk, *Diamond Electrochemistry*, Elsevier, Amsterdam, **2005**.
[4] B. B. Pate, *Surf. Sci.* **1986**, *165*, 83 – 142.
[5] H. Kawarada, *Surf. Sci. Rep.* **1996**, *26*, 205 – 259.
[6] D. B. Rebuli, P. Aggerholm, J. E. Butler, S. H. Connell, T. E. Derry, B. P. Doyle, R. D. Maclear, J. P. F. Sellschop, E. Sideras-Haddad, *Nucl. Instrum. Methods Phys. Res. Sect. B* **1999**, *158*, 701 – 705.■■ok?■■
[7] J. D. Lambert, *Trans. Faraday Soc.* **1936**, *32*, 452 – 462.
[8] W. Haenni, J. Gobet, A. Perret, L. Pupunat, Ph. Rychen, C. Comninellis, B. Correa, *New Diam. Front. C. Tec.* **2002**, *12*, 83 – 88.
[9] P. Rychen, L. Pupunat, W. Haenni, E. Santoli, *New Diam. Front. C. Tec.* **2002**, *13*, 109 – 117.
[10] M. Panizza, E. Brillas, C. Comninellis, *J. Environ. Eng. Manage.* **2008**, *18*, 139 – 153.■■reference not found?■■
[11] T. Yano, D. A. Tryk, K. Hashimoto, A. Fujishima, *J. Electrochem. Soc.* **1998**, *145*, 1870 – 1876.
[12] B. Hammer, L. B. Hansen, J. K. Nørskov, *Phys. Rev. Lett.* **1996**, *59*, 7413 – 7421 http://www.fysik.dtu.dk/campos.■■Please check the reference; URL leads to "page not found"■■
[13] D. Vanderbilt, *Phys. Rev. B* **1990**, *41*, 7892 – 7895.
[14] J. P. Perderw in *Electronic Structure of Solids* (Eds.: P. Ziesche, H. Eschrig), Akademie Verlag, Berlin, **1991**, p. 11.
[15] H. J. Monkhorst, J. D. Pack, *Phys. Rev. B* **1976**, *13*, 5188 – 5192.
[16] L. Bengtsson, *Phys. Rev. B* **1999**, *59*, 12301 – 12304.
[17] E. Santos, W. Schmickler, *ChemPhysChem* **2006**, *7*, 2282 – 2285.
[18] E. Santos, W. Schmickler, *Chem. Phys.* **2007**, *332*, 39 – 47.
[19] E. Santos, W. Schmickler, *Angew. Chem. Int. Ed.* **2007**, *46*, 8262 – 8265; *Angew. Chem.* **2007**, *119*, 8410 – 8413.
[20] E. Santos, M. Koper, M. W. Schmickler, *Chem. Phys.* **2008**, *344*, 195 – 201.
[21] E. Santos, K. Pötting, W. Schmickler, *Faraday Discuss.* **2009**, *140*, 209 – 218.■■ok?■■
[22] J. K. Kang, C. B. Musgrave, *J. Chem. Phys.* **2000**, *113*, 7582 – 7587.
[23] D. Petrini, K. Larsson, *J. Phys. Chem. C* **2007**, *111*, 795 – 801.
[24] N. Russo in *Structure and Reactivity of Surfaces* (Eds.: C. Morterra, A. Zecchina, G. Gosta), Elsevier, Amsterdam, **1989**.
[25] X. M. Zheng, P. V. Smith, *Surf. Sci.* **1992**, *262*, 219 – 234.
[26] S. Skokov, B. Weiner, M. Frenklach, *Phys. Rev. B* **1994**, *49*, 11374 – 11382.
[27] P. Badziag, W. S. Verwoerd, *Surf. Sci.* **1987**, *183*, 469 – 483.
[28] P. E. Pehrsson, T. W. Mercer, *Surf. Sci.* **2000**, *460*, 74 – 90.
[29] R. T. Morrison, R. N. Boyd, *Organic Chemistry*, Prentice Hall, Englewood Cliffs, New Jersey, **1992**.
[30] G. Zilibotti, S. Corni, M. C. Righi, *Phys. Rev. B* **2012**, *85*, 033406.
[31] B. Marselli, J. Garcia-Gomez, P. A. Michaud, M. A. Rodrigo, Ch. Comninellis, *J. Electrochem. Soc.* **2003**, *150*, D79 – D83.
[32] A. Kapalka, G. Foti, C. Comninellis, *Electrochim. Acta* **2009**, *54*, 2018 – 2023.
[33] E. Santos, A. Lundin, K. Pötting, P. Quaino, W. Schmickler, *Phys. Rev. B* **2009**, *79*, 235436.
[34] W. Schmickler, *J. Electroanal. Chem.* **1986**, *204*, 31 – 43.
[35] R. A. Marcus, *J. Chem. Phys.* **1956**, *24*, 966 – 980.
[36] N. S. Hush, *J. Chem. Phys.* **1958**, *28*, 962 – 972.
[37] D. Asthagiri, L. R. Pratt, J. D. Kress, M. A. Gomez, *Chem. Phys. Lett.* **2003**, *380*, 530 – 535.
[38] L. M. C. Pinto, E. Spohr, P. Quaino, E. Santos, W. Schmickler, *Angew. Chem. Int. Ed.* **2013**, *52*, 7883 – 7885; *Angew. Chem.* **2013**, *125*, 8037 – 8040.
[39] L. M. C. Pinto, P. M. Quaino, M. Arce, E. Santos, W. Schmickler, submitted.■■journal name? DOI? If possible, please provide full citation including page numbers■■

[40] A. M. Kuznetsov, *Charge Transfer in Physics, Chemistry and Biology*, Gordon & Breach, New York, **1995**.
[41] S. I. Pekar, *Untersuchungen über die Elektronentheorie der Metalle*, Akademie Verlag, Berlin, **1954**.
[42] S. I. Pekar, *Research in Electron Theory of Crystals*, USAEC, Washington D.C., **1963**.
[43] G. V. Burton, C. L. Greenstock, W. P. Helmann, A. B. Ross, *J. Phys. Chem. Ref. Data* **1988**, *17*, 513 – 886.
[44] A. Bard, R. Parsons, J. Jordan, *Standard Potentials in Aqueous Solutions*, Marcel Dekker, New York, **1985**.
[45] H. Gerischer, *Z. Phys. Chem. (Muenchen Ger.)* **1960**, *26*, 223 – 247; **1961**, *27*, 48 – 79.
[46] W. Schmickler, E. Santos, *Interfacial Electrochemistry 2nd ed.*, Springer, Berlin, **2010**, chapter 11.

Received: October 25, 2013
Revised: November 25, 2013
Published online on ■■ ■■, 2014

P. M. Quaino, W. Schmickler*

■■ – ■■

Oxygen-Terminated Diamond Electrodes in Alkaline Media: Structure and OH Generation

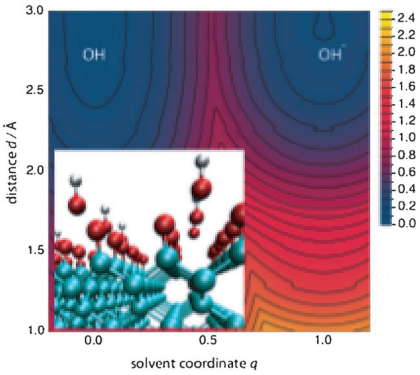

Not only a girl's best friend: Boron-doped diamond is important as an electrode material. Oxygen-terminated diamonds and the kinetics of OH generation in alkaline solutions on this type of surface are studied theoretically; this allows detailed structure and energetics characterization of the systems, as well as an understanding of the reaction dynamics that proceed in an outer-sphere mode.

Quaino/Schmickler - OH generation in oxygen-terminated BDD # electrodes @unlitoral @chemie de SPACE RESERVED FOR IMAGE AND LINK

ChemElectroChem is piloting a social networking feature involving Twitter, an online microblogging service that enables its users to send and read text-based messages of up to 140 characters, known as "tweets". Please check the pre-written tweet in the galley proofs for accuracy. Should you or your institute have a Twitter account, please let us know the appropriate username (e.g., @ChemElectroChem), and we will do our best to include this information in the tweet. This tweet will be posted to the journal's Twitter account upon online publication of your article.